Journal of Applied Mechanics and Technical Physics, Vol. 42, No. 2, pp. 237–242, 2001

APPROXIMATE MODELS OF EXHAUSTION OF A SUPERSONIC GAS JET INTO VACUUM

V. A. Shuvalov, O. A. Levkovich, and G. S. Kochubei

UDC 532.525.2:533.697.4

Approximate models for calculation of gas-dynamic parameters of supersonic jets escaping into vacuum are proposed. It is shown that the structural description and the spatial distribution of the parameters in the far field of the jet in the ideal and viscous approximations are in good agreement with the results of physical experiments and numerical solution of the problem.

The problem of the structure of a supersonic gas jet escaping into vacuum has various technological applications [1, 2]. The problem is usually solved numerically by the method of characteristics. Obtaining of such a solution is rather labor-consuming; therefore, approximate models are frequently used in engineering practice [1, 2]. These models have different degrees of correspondence to numerical and physical experiments but do not take into account viscous effects. Because of the boundary layer in the nozzle, the gas density in the peripheral part of the jet is significantly greater than the density calculated for the case of an inviscid (ideal) flow. The gas parameters at the jet periphery are used to determine the action of gas jets on various constructual elements of energy facilities, vacuum pumps, spacecraft surfaces, and other technical systems.

Viscous effects are taken into account in the model proposed in [3]. The accuracy of this model is determined to a large extent by an appropriate choice of the parameter m_z (the ratio of the gas discharge in the boundary layer to the total discharge of the gas) based on the results of a physical experiment or numerical analysis of the gas flow in the nozzle.

In the present paper, we propose two refined models, which allow one to increase the calculation accuracy of the parameters of a supersonic jet escaping from real nozzles into vacuum. The area of applicability of these approximate models is the far field (according to the estimates of [4], from $r/r_e \geqslant 10$, i.e., downstream of the boundary of continuity [5]), where the gas velocity in the jet increases and approaches the limiting value $V_{\max} = \sqrt{2\gamma RT_0/(\gamma-1)}$, and the streamlines are almost rectilinear. Here γ is the ratio of specific heats, R is the universal gas constant, T_0 is the stagnation temperature, r is the jet radius, and r_e is the nozzle-exit radius. As in [3], we assume that the far field of the jet may be simulated by a source with a pole at the center of the nozzle, the main mass of the gas and jet momentum are concentrated in the central core, where the gas flow is perfect, and viscous effects are manifested in the peripheral region. The results of the numerical solution of the problem or the data of a physical experiment may be used as a criterion of accuracy of approximate models.

In a polar system of coordinates with the origin at the center of the nozzle-exit cross section, the gas-density distribution in the far field of an axisymmetric supersonic jet may be represented in the following form (model No. 1):

Institute of Technical Mechanics, Ukrainian National Academy of Sciences, Dnepropetrovsk 49005, Ukraine. Translated from Prikladnaya Mekhanika i Tekhnicheskaya Fizika, Vol. 42, No. 2, pp. 62–67, March–April, 2001. Original article submitted May 12, 1999; revision submitted January 11, 2000.

0021-8944/01/4202-0237 $25.00

$$\frac{\rho(r,\theta)}{\rho_0} = \frac{\gamma+1}{2}\Big(1+\frac{k}{2\gamma}\Big)^{-1/(\gamma-1)}\Big(1+\frac{k}{2\gamma}-\gamma^{-1}\Big)\Big(\frac{r}{r_{\rm e}}\Big)^{-2}\Big(\cos\frac{\theta}{2}\Big)^{\beta_1}$$
$$\times\Big[1-m_{z_1}\Big(1-\frac{2+\beta_*}{2+\beta_1}\Big(\cos\frac{\theta}{2}\Big)^{\beta_*-\beta_1}\Big)\Big]. \qquad (1)$$

Here $k=\gamma(\gamma-1)\mathrm{M}_{\rm e}^2$ ($\mathrm{M}_{\rm e}$ is the Mach number at the nozzle exit) and θ is the angle between the radius-vector of the considered point of the jet and its centerline,

$$\beta_1=\frac{\mathrm{M}_{\rm e}}{\gamma(\gamma^2+1)}\,\beta,\qquad \beta=\frac{4C_F/C_{F,\max}}{1-C_F/C_{F,\max}},\qquad m_{z_1}=\frac{1}{2}\Big(1-\frac{C_F}{C_{F,\max}}\Big),$$

where

$$\frac{C_F}{C_{F,\max}}=C_{\rm con}C_{\rm d}C_V\Big(\frac{k}{k+2\gamma}\Big)^{0.5}+\Big(1+\frac{k}{2\gamma}\Big)^{-\gamma/(\gamma-1)}\frac{A_{\rm e}}{A_*}\,C_{F,\max}^{-1},$$

$$C_{F,\max}=\frac{2\gamma}{\sqrt{\gamma^2-1}}\Big(\frac{2}{\gamma+1}\Big)^{\gamma/(\gamma-1)},\qquad C_{\rm con}=\frac{1+\cos\theta_{\rm e}}{2},$$

C_F is the thrust coefficient of a real nozzle, $C_{F\,\max}$ is the thrust coefficient for inviscid exhaustion of the jet into vacuum, $C_{\rm con}$ is the conicity coefficient of the nozzle, $C_{\rm d}$ is the discharge coefficient, C_V is the velocity coefficient, and $\beta_*=\beta$ for $A_{\rm e}/A_*=1$ ($A_{\rm e}$ is the cross-sectional area of the nozzle exit and A_* is the area of the nozzle throat). In an inviscid flow, we have $C_F/C_{F,\max}=1$ and $m_z=0$.

Kuluva and Hosack [6] obtained the following relation for the discharge coefficient $C_{\rm d}$:

$$C_{\rm d}=1-\Big(\frac{r_{\rm c}}{r_*}\Big)^{0.25}\frac{0.97+0.86\gamma}{\sqrt{\mathrm{Re}_*}}. \qquad (2)$$

Here $0\leqslant r_{\rm c}/r_*\leqslant 2$, $50<\mathrm{Re}_*<10^5$, $r_{\rm c}$ is the curvature radius of the profile in the nozzle-throat cross section, r_* is the radius of the nozzle-throat cross section, and Re_* is the Reynolds number in the nozzle-throat cross section.

In [7], the discharge coefficient is represented as the approximation

$$C_{\rm d}=0.998-2\delta_*/r_*, \qquad (3)$$

where δ_* is the displacement thickness.

For real nozzles, the velocity coefficient is determined by the relation [8]

$$C_V=\frac{(1-T_{\rm e}/T_0)^{0.5}}{\sqrt{k/(k+2\gamma)}} \qquad (4)$$

($T_{\rm e}$ is the flow temperature at the nozzle exit). In the adiabatic flow regime, we have

$$C_V=\sqrt{1+\frac{2}{\gamma}\,(C_{\rm d}-1)}. \qquad (5)$$

Figure 1 shows the measured and calculated values of $C_{\rm d}$ (curve 1 and points 2–5) and $T_{\rm e}/T_0$ (points 6 and 7, respectively) for $10^{-1}\leqslant\mathrm{Re}_*\leqslant 10^6$ and $\gamma=1.4$. Curve 1 refers to the averaged data of the experiment [9], points 2 to the data of [10], 3 to the calculation of [11], 4 to approximation (2) for $r_{\rm c}/r_*=1.5$, 5 to approximation (3) for the data of [12], 6 to the data of [10], and 7 to the data of [12] for a conical nozzle with an expansion $A_{\rm e}/A_*=100$ and inclination of the nozzle exit to its axis $\theta_{\rm e}=15^\circ$ ($T_0=1100$ K, and $\gamma=1.37$). The measurements and calculations performed in a wide range of stagnation parameters for different conditions of gas-jet exhaustion from nozzles may be used to evaluate the coefficients $C_{\rm d}$ and C_V. Taking into account the numerical data of [10, 13], approximations (2)–(5), in fact, determine the areas of applicability of model No. 1: $\mathrm{M}_{\rm e}\geqslant 1$ ($1\leqslant A_{\rm e}/A_*\leqslant 10^3$) and $50\leqslant\mathrm{Re}_*\leqslant 10^6$. The density distribution across the jet (with respect to the axis of symmetry) in the far field is almost independent of r and is determined by the ratio $\rho/\rho_a=\rho(r,\theta)/\rho(r,0)$.

If the characteristics of real nozzles (coefficients $C_{\rm d}$ and C_V) are unknown, the jet parameters in the far field can be determined using model No. 2:

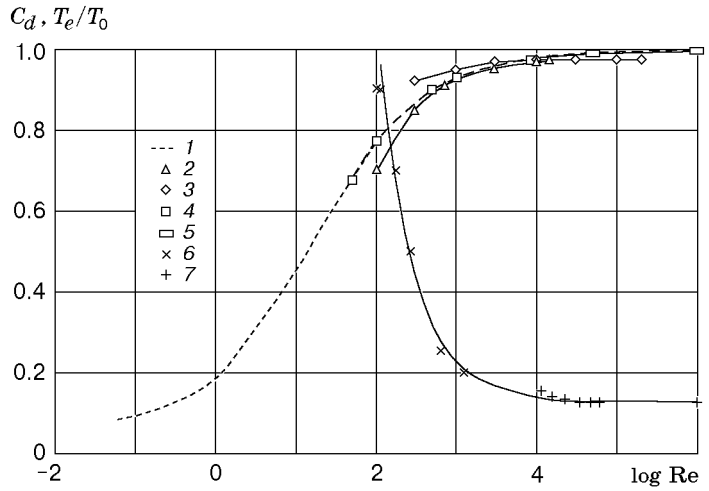

Fig. 1

$$\frac{\rho(r,\theta)}{\rho_0} = \frac{\gamma+1}{2}\Big(1+\frac{k}{2\gamma}\Big)^{-1/(\gamma-1)}\Big(1+\frac{k}{2\gamma}-\gamma^{-1}\Big)\Big(\frac{r}{r_{\rm e}}\Big)^{-2}$$

$$\times\,(\cos\theta)^{\beta_2}\Big[1-m_{z_2}\Big(1-\frac{2+\beta_*}{2+\beta_2}\,\frac{(\cos(\theta/2))^{\beta_*}}{(\cos\theta)^{\beta_2}}\Big)\Big], \tag{6}$$

where

$$\beta_2 = 1.249\exp(0.418\,{\rm M_e}); \qquad m_{z_2} = \frac{1}{\xi}\Big(1-\frac{C_F}{C_{F,\max}}\Big);$$

$$\frac{C_F}{C_{F,\max}} = \frac{1+\cos\theta_{\rm e}}{2}\Big(\frac{k}{k+2\gamma}\Big)^{0.5} + \Big(1+\frac{k}{2\gamma}\Big)^{-\gamma/(\gamma-1)}\frac{A_{\rm e}}{A_*}\,C_{F\max}^{-1}; \quad \xi = 63.1\sqrt{\frac{\gamma(\gamma-1)}{{\rm M_e}}} - 13.7.$$

The correctness of model Nos. 1 and 2 is illustrated in Fig. 2, which shows the angular distributions of density $\rho(r,\theta)/\rho(r,0) = \rho/\rho_a$ for a supersonic gas jet escaping from a real nozzle into vacuum.

The relation

$$\frac{\rho}{\rho_a} = \Big[1-m_{z_1}\Big(1-\frac{2+\beta_*}{2+\beta_1}\Big)\Big(\cos\frac{\theta}{2}\Big)^{\beta_*-\beta_1}\Big]\Big(\cos\frac{\theta}{2}\Big)^{\beta_1}\Big/\Big[1-m_{z_1}\Big(1-\frac{2+\beta_*}{2+\beta_1}\Big)\Big] \tag{7}$$

corresponds to model No. 1, and the next relation corresponds to model No. 2:

$$\frac{\rho}{\rho_a} = \Big[1-m_{z_2}\Big(1-\frac{2+\beta_*}{2+\beta_2}\Big)\Big(\cos\frac{\theta}{2}\Big)^{\beta_*}\Big/\Big(\cos\theta\Big)^{\beta_2}\Big]\Big(\cos\theta\Big)^{\beta_2}\Big/\Big[1-m_{z_2}\Big(1-\frac{2+\beta_*}{2+\beta_2}\Big)\Big] \tag{8}$$

Figure 2a shows the density distribution in the jet cross section $r/r_{\rm e} = 70$ for ${\rm M_e} = 6.9$, $\theta_{\rm e} = 15^\circ$, and $\gamma = 1.4$. Points 1 correspond to the numerical solution of the problem by the method of characteristics for a viscous flow [3]; curve 2 refers to the values calculated by Eq. (7) for $C_{\rm d} = 0.989$ and $C_V = 0.981$. The values of $C_{\rm d}$ and C_V are determined for conditions of hydrazine exhaustion from a conical nozzle for $\theta_{\rm e} = 15^\circ$, $A_{\rm e}/A_* = 100$, $T_0 = 1100$ K, and ${\rm Re}_* \approx 5.9\cdot 10^4$ [8, 12]. Curve 3 shows the results obtained by model No. 2 [relation (8) for a viscous flow], curve 4 refers to the results obtained by the model proposed in [3], and curve 5 corresponds to the results obtained by model No. 2 [relation (8) for an ideal flow for $m_{z_2} = 0$].

Figure 2b shows the angular distribution of the normalized density of the gas in the far field of a supersonic jet escaping into vacuum for ${\rm M_e} = 4.5$, $\theta_{\rm e} = 15^\circ$, and $\gamma = 1.4$. Points 1 correspond to the experimental data of [1] for ${\rm Re}_* = 6.5\cdot 10^4$ and $r/r_{\rm e} > 10$, curve 2 refers to the results obtained by model No. 1 [Eq. (7)], curve 3 was obtained by approximation (8), and curve 4 was plotted using Eq. (8) for an inviscid approximation for $m_{z_2} = 0$.

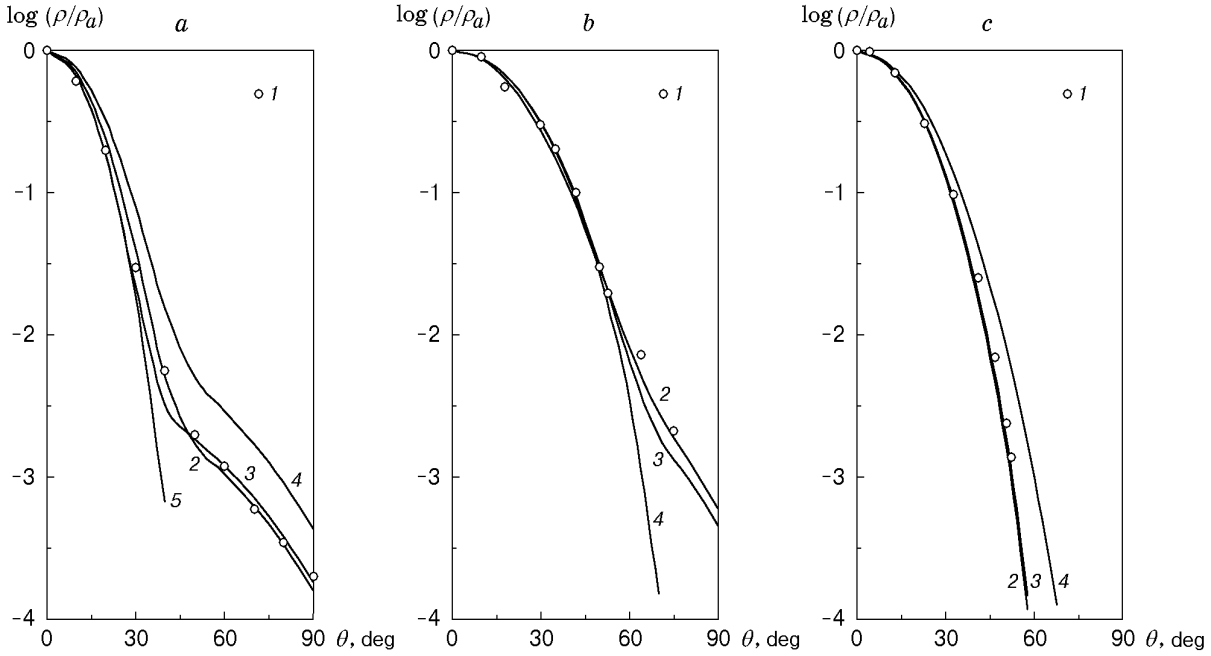

Fig. 2

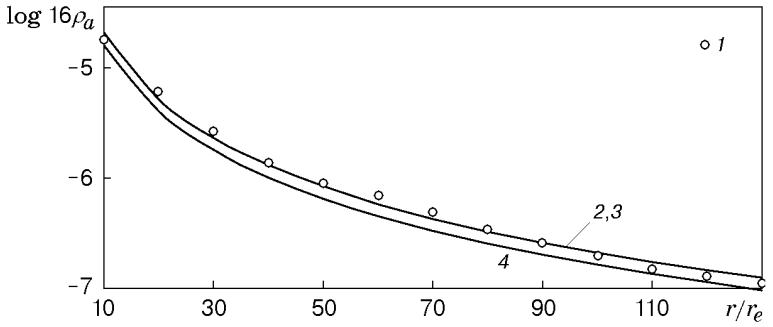

Fig. 3

A comparison of numerical data for an inviscid flow, which were obtained by the method of characteristics [14] for $M_e = 5.0$, $\gamma = 1.4$, $\theta = 15°$, and $r/r_e = 78$ (Fig. 2c), with the calculation results by Eqs. (7) and (8) shows that the angular distributions of the gas density are adequately described by model Nos. 1 and 2 in the case of ideal exhaustion. Points 1 in Fig. 2c correspond to the calculations by the method of characteristics [14], curve 2 is plotted by Eq. (8) for $m_{z_2} = 0$, curve 3 is plotted by the model of inviscid exhaustion [15]

$$\frac{\rho(r,\theta)}{\rho_0} = 0.5k\Big(1+\frac{k}{2\gamma}\Big)^{-1/(\gamma-1)}\Big(\frac{r}{r_e}\Big)^{-2}(\cos\theta)^k, \tag{9}$$

and curve 4 is plotted for $m_z = 0$ using the model proposed in [3].

The gas-density distributions obtained by model Nos. 1 and 2 are closer to the calculation results by the method of characteristics and the physical experiment than those obtained using the model proposed in [3]. This is illustrated by the data for angular distributions of density in Fig. 2 and axial distributions of density $\rho_a = \rho(r,0)$ in Fig. 3.

In Fig. 3, points 1 correspond to the results of the numerical solution of the problem by the method of characteristics for a viscous flow for $M_e = 6.9$, $\theta_e = 15°$, and $\gamma = 1.4$, which were obtained in [3], curve 2 refers

to the results obtained by model No. 1, curve 3 shows the results obtained by model No. 2, and curve 4 refers to the results obtained by the model proposed in [3] for $m_z = 0.07$ (curves 2 and 3 almost coincide). Similar dependences for an inviscid flow for $\mathrm{M_e} = 5.0$, $\gamma = 1.4$, $\theta = 15°$, and $10 \leqslant r/r_\mathrm{e} \leqslant 250$, which were obtained by the method of characteristics [14], by model No. 2 for $m_{z_2} = 0$, and by approximation (9), are also in good agreement. Viscous effects in the case of supersonic exhaustion of a gas into vacuum are manifested in the peripheral part of the jet for $\theta > 40°$ and $\rho/\rho_a < 10^{-2}$ (curve 5 in Fig. 2a and curve 4 in Fig. 2b). In the axial region ($\theta \leqslant 40°$), the solutions for the viscid and inviscid flows almost coincide. The main mass of the gas expands inside the cone whose half-angle is smaller than $0.5\theta_\mathrm{max}$. The limiting angle of jet expansion is determined by the relation $\theta_\mathrm{max} = \psi(\mathrm{M}) - \psi(\mathrm{M_e}) + \theta_\mathrm{e}$, $\mathrm{M} = \infty$, where $\psi(\mathrm{M})$ is the Prandtl–Mayer function. The influence of the angle θ_e on the Mach number distribution on the jet axis and in its vicinity is mainly manifested near the nozzle exit and becomes insignificant further downstream [1, 2]. Therefore, for the axial distribution of Mach numbers, we can use the relation

$$\frac{\mathrm{M}(x)}{\mathrm{M_e}} = \sqrt{\frac{2\gamma}{k}}\left(\left\{\frac{\gamma+1}{2\gamma}\Big(1+\frac{k}{2\gamma}\Big)^{-1/(\gamma-1)}\Big[\gamma\Big(1+\frac{k}{2\gamma}\Big)-1\Big]\Big(\frac{x}{r_\mathrm{e}}\Big)^{-2}\right\}^{1-\gamma} - 1\right)^{0.5}. \tag{10}$$

The values of $\mathrm{M}(x)/\mathrm{M_e}$ obtained by Eq. (10) for $\mathrm{M_e} = 5.0$ and $\gamma = 1.4$ correspond to the numerical solution of the problem by the method of characteristics [14] with an error of less than the streamwise distribution of density ρ_a ($r = x$ and $\theta = 0$) obtained by formulas (1) and (6).

In the case of gas exhaustion into vacuum, the flow regime in the jet varies from continuum to free-molecular. Based on the above considerations, the boundary of flow continuity in the axial zone may be found by the formula [16]

$$\frac{r_\mathrm{bound}}{r_\mathrm{e}} = \left[\frac{2r_\mathrm{e}}{l_0}\Big(\frac{\gamma-1}{\pi\gamma}\Big)^{0.5}\right]^{1/(N+1)}\Big(0.5k\,\frac{\rho_\mathrm{e}}{\rho_0}\,(\cos\theta)^k\Big)^{0.5}, \tag{11}$$

where l_0 and ρ_0 are the mean free path and the gas density upstream of the nozzle, respectively, $N = \nu(\gamma-1)$, $\nu = 2(1-\omega)$, and ω is the power index in the viscosity versus temperature dependence.

Taking into account relations (11), one can use the approximate models proposed to predict the spatial distribution of the gas density and Mach numbers in the far field ($r/r_\mathrm{e} > r_\mathrm{bound}/r_\mathrm{e}$) of a supersonic jet with viscid and inviscid exhaustion into vacuum with an accuracy corresponding to the numerical solution of the problem by the method of characteristics and to determine the force and thermal action of the jets on targets.

REFERENCES

1. V. S. Avduevskii, É. Ya. Ashratov, A. V. Ivanov, and U. G. Pirumov, *Supersonic Nonisobaric Gas Jets* [in Russian], Mashinostroenie, Moscow (1985).
2. V. G. Dulov and G. A. Luk'yanov, *Gas Dynamics of Exhaustion Processes* [in Russian], Nauka, Novosibirsk (1984).
3. E. Meier, J. Hermel, and A. V. Rodgers, "Loss of thrust due to the interaction of the exhaust jet with constructional elements of an orbital flying vehicle," *Aerokosm. Tekh.*, No. 8, 118–126 (1987).
4. G. Dettleff, R.-D. Doetcher, C. Dankert, et al., "Attitude control thruster plume flow modelling and experiments," *J. Spacecraft Rocket*, **23**, No. 5, 477–481 (1986).
5. A. L. Stasenko, "Criteria for the continuum flow in a freely expanding jet," *Inzh.-Fiz. Zh.*, **16**, No. 1, 9–14 (1969).
6. N. M. Kuluva and G. A. Hosack, "Supersonic nozzle discharge coefficients at low Reynolds numbers," *AIAA J.*, **9**, No. 9, 1876–1879 (1971).
7. M. W. Milligan, "Nozzle characteristics in the transitional flow regime between continuum and free-molecular flow," *AIAA J.*, **2**, No. 6, 1088–1092 (1964).
8. H. W. Emmons (ed.), *Fundamentals of Gas Dynamics*, Princeton University Press (1958).

9. P. F. Massier, L. H. Back, M. B. Noel, and F. Sahel, "Viscous effects of the flow coefficient for a supersonic nozzle," *AIAA J.*, **8**, No. 3, 605–607 (1970).
10. D. E. Rothe, "Electron-beam studies of viscous flow in supersonic nozzles," *AIAA J.*, **9**, No. 5, 804–811 (1971).
11. W. J. Rae, "Some numerical results on viscous low-density nozzle flows in the slender-channel approximation," *ibid.*, pp. 811–820.
12. R. Kushida, J. Hermel, S. Apfel, and M. Zydowicz, "Performance of a high-area-ratio nozzle for a small rocket thruster," *J. Propulsion Power*, **3**, No. 4, 329–334 (1987).
13. S. M. Liang, K. S. Huang, and K. C. Chen, "Numerical study of low-thrust nozzles for satellites," *J. Spacecraft Rockets*, **33**, No. 5, 693–699 (1996).
14. G. I. Averenkova, E. A. Ashratov, T. G. Volokonskaya, et al., *Supersonic Jets of an Ideal Gas* [in Russian], Izd. Mosk. Univ., Moscow (1970).
15. L. Roberts and J. C. South, Jr., "Comments on exhaust flow field and surface impingement," *AIAA J.*, **2**, No. 5, 971–973 (1964).
16. V. M. Antokhin, Yu. P. Balashov, Yu. I. Semenov, et al., "Investigation of the flow around the 'Apollo' spacecraft," *Mekh. Zhidk. Gaza*, No. 3, 124–133 (1977).